Available online at www.sciencedirect.com
ScienceDirect
C. R. Geoscience 340 (2008) 298–305
COMPTES RENDUS GEOSCIENCE
http://france.elsevier.com/direct/CRAS2A/

Geomaterials (Mineralogy)

Thermal and hydrothermal influence of magmatic emissions on embedding clays of the Upper Cretaceous of the Tunisian eastern margin and the Pelagic Sea

Hanene Mattoussi Kort *, Aicha Beji Sassi, Nejia Laridhi Ouazaa

University of Tunis El Manar, Faculty of Sciences, Department of Geology, Crystalline Petrology and Sedimentary Unit, Campus 2092 Manar-II, Tunis, Tunisia

Received 26 March 2007; accepted after revision 7 January 2008
Available online 7 March 2008

Presented by Georges Pédro

Abstract

During the Upper Cretaceous, magmatic manifestations took place in the Tunisian eastern margin and the Pelagic Sea. Intrusions are mainly microdolerites, whether they are accompanied or not by basaltic lava flows, breccia, pyroclastic facies. Thermal influence of the intrusions on the embedding sedimentary deposits resulted in a set of transformations. Temperature elevation and hydrothermal conditions led to the neoformation of chlorite and mixed-layered illite–chlorite near to the intrusions and below the lava flows. Illite crystallinity is improved close to the microdolerites and basaltic lava flows. ***To cite this article: H. Mattoussi Kort et al., C. R. Geoscience 340 (2008).***

Résumé

Influence thermique et hydrothermale des émissions magmatiques sur les minéraux argileux du Crétacé supérieur de la marge orientale de la Tunisie. Au cours du Crétacé supérieur, des manifestations magmatiques ont eu lieu sur la marge orientale de la Tunisie (Sahel et mer Pélagienne). Elles sont liées à l'ouverture des grabens de Syrte et au coulissage de l'Ibérie vers le sud-est entre l'Aptien et le Sénonien. Il s'agit essentiellement d'intrusions microdoléritiques, accompagnées ou non de coulées basaltiques, de faciès bréchiques et pyroclastiques. La mise en place des intrusions et des coulées de basalte a été accompagnée d'un apport de chaleur et de migrations de fluides. Ces manifestations thermiques ont conduit à la néoformation de la chlorite, d'interstratifiés illite–chlorite, au voisinage des intrusions et sous les coulées de basalte. Elles ont aussi conduit à une amélioration de la cristallinité de l'illite au voisinage immédiat des manifestations magmatiques. ***Pour citer cet article : H. Mattoussi Kort et al., C. R. Geoscience 340 (2008).***

Keywords: Clay minerals; Cretaceous; Tunisia; Thermal influence; Magmatic intrusion; Chlorite

Mots clés : Influence thermique ; Minéraux argileux ; Crétacé supérieur ; Tunisie ; Intrusion magmatique ; Chlorite

* Corresponding author.
E-mail address: mkhanen@yahoo.fr (H. Mattoussi Kort).

1631-0713/$ – see front matter © 2008 Académie des sciences. Published by Elsevier Masson SAS. All rights reserved.
doi:10.1016/j.crte.2008.01.004

1. Introduction

The current study addresses thermal effects generated by an intrusive magmatic activity onto embedding sedimentary deposits of the Tunisian Eastern margin (Fig. 1). This margin comprises the area between the Cap Bon in the North and the Gabes in the South. The study is based on subsurface data and samples recovered in the oil wells of this area. Samples were collected all along the drillings and in tighten steps near the magmatic intervals. The study aim is to appraise the impact of both heat and chemical elements income – relevant to the magmatic rocks setup – on the neoformation of new mineral phases and the improvement of their crystallinity degree.

2. Geological frame

2.1. Eastern margin structure

The geological structure of the eastern margin of Tunisia results from two main tectonic behaviours:

- successive rifting, with north–south to NE–SW extensions along the Trias, Jurassic and Lower Cretaceous, which led to series of horsts, grabens and semi-graben structures;
- the migration of the African plate towards Eurasia during the Upper Cretaceous and the Cenozoic initiated NW–SE compression and formation of the Atlasic mountain folding [8,12,26].

2.2. Magmatic manifestations during the Upper Cretaceous

Subsurface magmatic rocks have been recovered in almost all the drillings across the Upper Cretaceous series of the eastern margin of Tunisia (Fig. 1). There are three main types of magmatic rocks [16,17,23] (Fig. 2):

- microdoleritic intrusions typical of fissural magmatic activity, forming dykes and sills;
- lava flows interstratified within the Cretaceous deposits;
- pyroclastic products (pumice, tufas) bearing witness to a synsedimentary explosive volcanic activity, which appeared during the Senonian. The pyroclastic fragments are composed of pumice debris, vitreous shards, or volcanic ashes amended by carbonate. The microscopic study shows that rocks are formed of pumice and scoria and pumice debris cemented by carbonate that may reach 40% of the rock. They correspond to a volcanism situated in carbonated sedimentation environment. Volcanoclastites are rare crystals and are affected by an intense post-magmatic transformation that made impossible their identification.

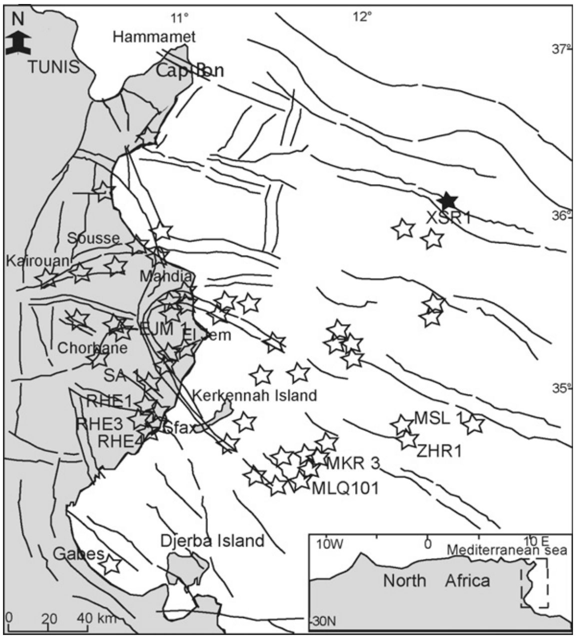

Fig. 1. Tectonic map showing the Cretaceous magmatism distribution in the study area: wells with magmatic manifestation (empty star); reference well without magmatism (full star). EJM1 (Eljem 1); SA1 (Sidi Abdellah 1); RHE1 (Rhemoura 1); RHE4 (Rhemoura 4); RHE3 (Rhemoura 3); MLQ101 (Mélquart 101); MKR3 (Miskar 3); MSL1 (M'sella 1); ZHR1 (Zohra 1); XSR1 (reference well).

Fig. 1. Carte tectonique montrant la distribution du magmatisme crétacé dans la zone d'étude : puits avec manifestation magmatique (étoiles blanches) ; puits de référence sans magmatisme (étoile noire). EJM1 (Eljem 1) ; SA1 (Sidi Abdellah 1) ; RHE1 (Rhemoura 1) ; RHE4 (Rhemoura 4) ; RHE3 (Rhemoura 3) ; MLQ101 (Mélquart 101) ; MKR3 (Miskar 3) ; MSL1 (M'sella 1) ; ZHR1 (Zohra 1); XSR1 (puits de référence).

2.3. Upper Cretaceous sedimentary deposits

The sedimentary facies of the Upper Cretaceous are strictly related to palaeogeographic directions guided by the basin structure. The transgression started during the Aptian and went on during the Cenomanian. The transgressive episode carried on and the facies became increasingly carbonated during the Coniacian–Santonian. During the Campanian–Maastrichtian, the transpressive facies became mainly carbonated and most often chalky. This sedimentation was characterised [22] by two high zones separated by a NW–SE trending

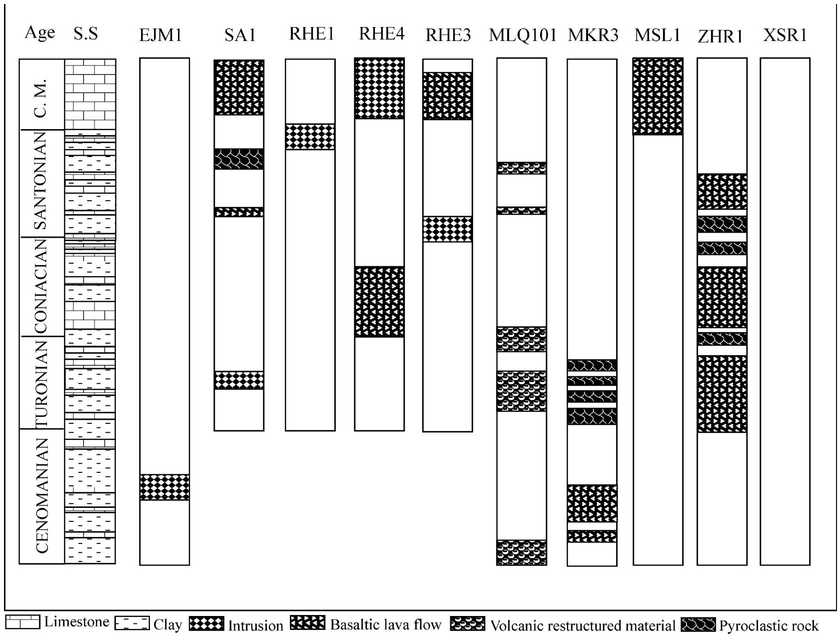

Fig. 2. Distribution and nature of magmatism of eastern Tunisia and the Pelagic Sea wells in the Upper Cretaceous. S.S.: Synthetic section of the Upper Cretaceous lithology.

Fig. 2. Distribution et nature du magmatisme dans les puits de l'Est de la Tunisie et de la mer Pélagienne, au Crétacé supérieur. S.S : coupe synthétique de la lithologie au Crétacé supérieur.

subsidence zone. This structure influenced sedimentary rates during the Upper Cretaceous.

2.4. The primary clay mineral suite

The clay mineral suite of the Upper Cretaceous formations outcropping in central Tunisia has been explored by numerous authors [1,14,24,26]. The authors point to the predominance of the smectite, together with little kaolinite and a very low amount of illite. It seems therefore that away from the occasional thermal influence of magmatic activity and the effect of burial diagenesis, the Upper Cretaceous reveals smectite dominance associated with illite and kaolinite. The authors interpret the predominance of smectite coming with small amount of kaolinite and illite as detrital heritage of the mineralogical suite, indicating tectonic stability during this period.

3. Methods

The clay minerals ($< 2\,\mu m$ fraction) have been analysed by X-ray diffraction. Clay samples collected in the cuttings were carefully selected under binocular magnifier to avoid contamination with well mud and fallouts. They were rinsed several times with water and then dried in free air. Consolidated samples were crushed. Calcareous samples were treated with 0.1 N chlorhydric acid. Then samples were washed and centrifuged. We used a pipette to collect the suspension in the upper slice. We put the suspension on a glass slide and let it evaporate at ambient air. The oriented clay aggregates were analysed by a Philips Panalytical diffractometer (XPERT-PRO) with a cobalt anticathode, a step size [0.017° 2θ], with X-rayed angular domain [0–35° 2θ] and step time [20.0298 s]. The oriented aggregates were run at air-dried state (after drying in ambient temperature), after saturation with ethylene glycol, and heated at 500 °C during 2 hours. Minerals are defined following the position of reflections (001) on the three diffractograms. Semi-quantitative estimation of the clay minerals was done based on the relative surface of the main peak of each mineral (air-dried X ray diffractogramm). Error odds are of 5%. SEM microscopy was performed on some samples to investigate clay minerals' morphologies.

4. Sampling

More than 200 samples were analyzed. Two sampling series were accomplished:

- packed samples in the vicinity of the magmatic material contact;
- more spaced samples away from the magmatic occurrences to determine the influence of magmatic bodies on embedding argillaceous sediments.

The analyzed cuttings are of average size (a few centimetres). Herein we examine three wells considered the most representative:

- a reference well, Ksar-1 (XSR1), without magmatic intrusion or emission;
- Rhemoura-3 (RHE3) well goes through a basalt flow layer in the upper part and a microdolerite sill at depth;
- Miskar-3 (MKR3) displays magmatic emission in the upper part, but several basaltic layer and pyroclastic layers in depth.

5. Results

5.1. Clay mineral series

Two main clay mineral suites have been identified:

- a relative simple one mainly composed of smectite, coming with minor amounts of kaolinite and illite (Fig. 3);
- another set of samples, showing suites predominantly formed of chlorite and mixed-layered illite–chlorite (Fig. 4).

5.1.1. Reference well XSR1, without magmatic rocks

Analysed samples (collected between 1370 and 1540 m) belong to an alternation of claystone and limestone of Turonian, Coniacian, Santonian, and Cenomanian age. The clay mineral suite is composed of kaolinite, illite, and smectite. Smectite (70 to 80%) is always prevalent, whereas kaolinite (5 to 15%) and illite (7 to 18%) are less important (Fig. 5). The lack of chlorite and mixed-layered illite–chlorite has to be noticed.

5.1.2. Well RHE3, with two magmatic intervals

The first interval is a basaltic lava flow (crosscut between 2531 and 2593 m) occupying a large part of the Abiod formation of Campanian–Maastrichtian age (Fig. 6). The basalt flow rests on whitish microcrystalline limestone and is covered by dark grey claystone that is mainly composed of smectite (70 to 80%), kaolinite (6 to 20%) and illite (6 to 10%). The absence of the chlorite and the mixed-layered illite–chlorite has to be noticed in this interval. The second magmatic interval (crosscut between 2671 m and 2691 m) is a microdoleritic-textured intrusion. This intrusion is embedded in Coniacian–Santonian clays and limestones. The analysed samples are located at both sides of the intrusion. Their clay fractions show mixed-layered illite–chlorite (37% to 60%) associated with chlorite (13% to 30%) and with illite (2% to 24%). The presence of kaolinite with proportions ranging from

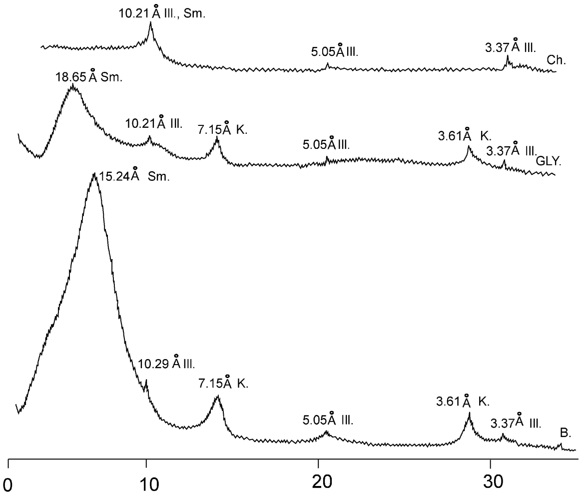

Fig. 3. X-ray diffractogramm for XSR1 well (1370 m). B.: Air-dried preparation; GLY.: EG-solvated preparation; CH.: heated preparation.

Fig. 3. Diffractogramme RX pour le puits XSR1 (1370 m) (section non intrudée). B. : préparation par séchage de l'air ; GLY. : préparation à l'éthylène glycol ; CH. : préparation chauffée.

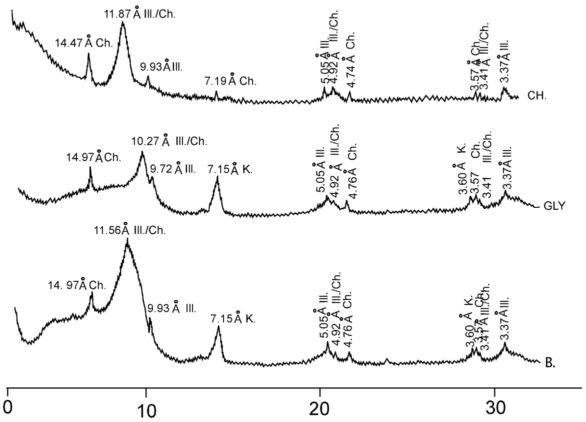

Fig. 4. X-ray diffractogramm for MKR3 well (3910 m). B.: Air-dried preparation; GLY.: EG-solvated preparation; CH.: heated preparation.

Fig. 4. Diffractogramme RX pour le puits MKR3 (3910 m) (avec émission magmatique). B. : préparation par séchage de l'air; GLY. : préparation à l'éthylène-glycol ; CH. : préparation chauffée.

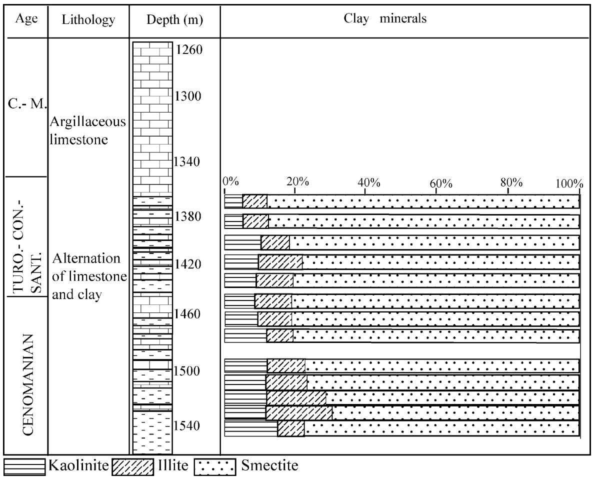

Fig. 5. Mineralogy of clay minerals of Upper Cretaceous sedimentary series in the XSR1 well.

Fig. 5. Composition argileuse de la série sédimentaire du Crétacé supérieur dans le puits XSR1, sans émission magmatique.

5 to 25% and the absence of smectite has to be noticed. Chlorite is slightly swelling with reflection (001) shifting from 14 to 14.95 Å by ethylene glycol solvation. The clay mineral suite shows an increase in chlorite content when coming closer to the intrusion. In fact, the samples in immediate contact with the intrusion (2672 m and 2694.5 m) reveal the highest chlorite content.

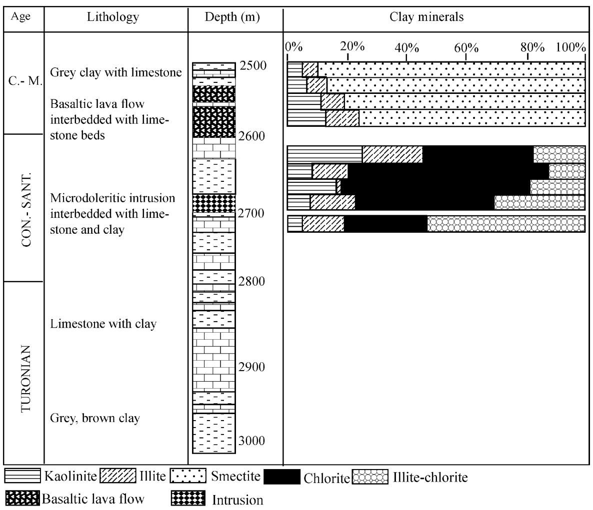

Fig. 6. Mineralogy of clay minerals of Upper Cretaceous sedimentary series in the RHE3 well.

Fig. 6. Composition argileuse de la série sédimentaire du Crétacé supérieur dans le puits RHE3, avec émission magmatique.

5.1.3. Well MKR3, with various magmatic activities

There are pyroclastic layers alternating with argillaceous limestones, as well as basaltic lava flows embedded in biomicrites and argillaceous limestones. There are two distinct clay mineral suites (Fig. 7). On either sides of the pyroclastic layer, the clay mineral suite is dominated by kaolinite (55% to 67%) associated with illite (9% to 35%) and smectite (9% to 28%). The lack of chloritic minerals has to be quoted. The clay minerals below the basaltic lava are composed of mixed-layered illite–chlorite (49% to 21%), chlorite (25% to 4%) and kaolinite, which increases away from the lava flow (from 7% to 38%). Illite contents range from 15% to 36%. Smectite is almost lacking; it has been detected only in two samples (3% and 2% at depths of 3920 and 3936 m, respectively). We notice that chlorite and mixed-layered illite–chlorite contents decrease when moving away from the basaltic lava flow,

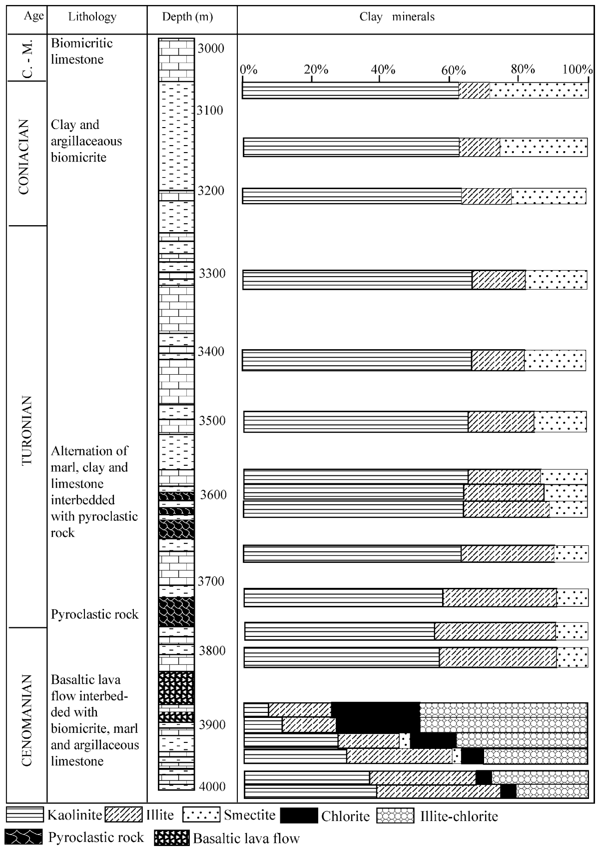

Fig. 7. Mineralogy of clay minerals of Upper Cretaceous sedimentary series in the MKR3 well.

Fig. 7. Composition argileuse de la série sédimentaire du Crétacé supérieur dans le puits MKR3, avec émission magmatique.

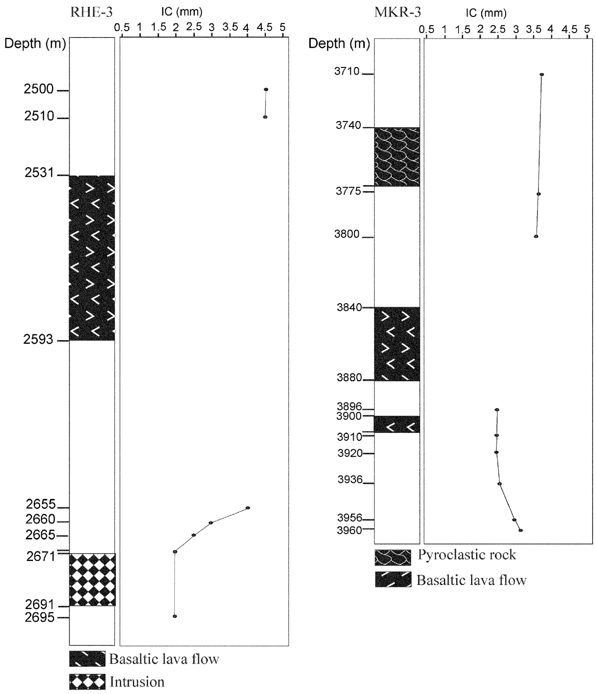

Fig. 8. Variation of the illite crystallinity index (IC) according to the illites' positions compared with microdoleritic intrusions in RHE3 well and with the basaltic lava flow in MKR3 well.

Fig. 8. Variation de l'indice de cristallinité de l'illite (IC) d'après la position des illites par rapport à l'intrusion microdoléritique dans le puits RHE3 et à la coulée de lave basaltique dans le puits MKR3.

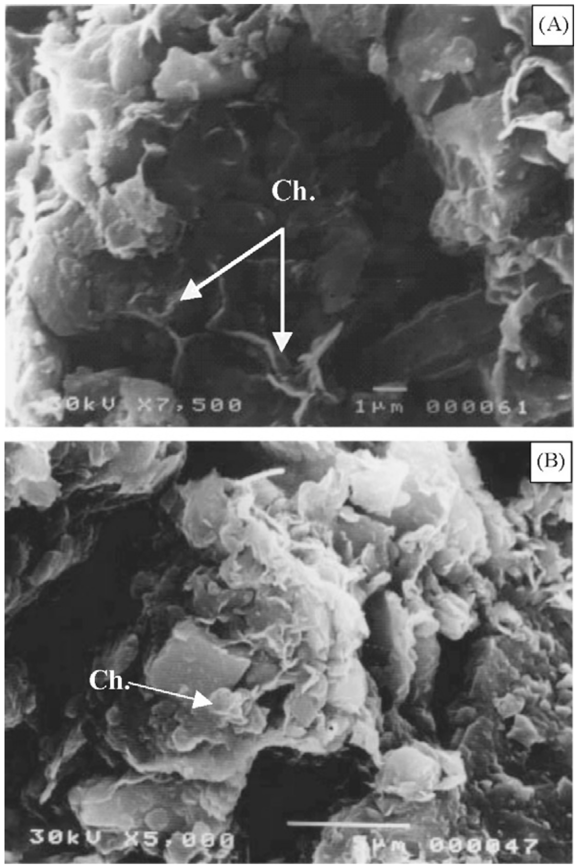

Fig. 9. Morphology of chlorite observed through scanning electron microscopy (SEM): (**A**) in RHE3 (2670 m), (**B**) in MKR3 (3910 m).

Fig. 9. Morphologie de la chlorite observée au microscope électronique à balayage (MEB) : (**A**) dans le puits RHE3 (2670 m), (**B**) dans le puits MKR3 (3910 m).

whereas kaolinite and illite contents increase in the meantime.

Chlorite and mixed-layered illite–chlorite minerals are bound to the magmatic intrusions (well RHE3) and the sole of the basaltic flow (well MKR3). There is no noteworthy change in the clay mineral series above the basalt flows (well RHE3) and near the pyroclastic deposits; in this latter configuration, clay mineral assemblages remain similar to those of the common detrital clay mineral series known elsewhere in the Upper Cretaceous of Tunisia, consisting of kaolinite, illite, and smectite, without chloritic minerals. The latter are directly bound to the emplacement of magmatic lavas.

5.2. Illite crystallinity

Special attention has been paid to the evolution of the illite crystallinity along the wells, by measurement of the width at half-height of the (001) reflexion of illite (EG solvated preparation) [5,10,15].

In the reference well XSR1, the (001) illite peak shows a width at half-height between 3.5 mm at 1540-m depth and 4.8 mm at 1440-m depth.

In well RHE3, illite crystallinity is rather low in the samples below the basaltic lava flow (around 2500-m depth) with a width at half-height of the (001) illite peak of about 4.5 mm (Fig. 8). Coming closer to the microdoleritic intrusion, illite crystallinity is improved, as shown by the decrease of its width at half-height (2.0 mm for samples between 2670 and 2695 m).

In well MKR3 (Fig. 9), samples at 3710 m and 3775 m have been collected at both top and bottom sides of the pyroclastic products. The measures of the crystallinity index are respectively 3.7 and 3.6 mm in this interval. The sample directly below the basaltic lava flow, at 3896-m depth, shows a higher illite crystallinity, with a half-height width of 2.5 mm. Moving away from the basalt layer, towards 3960-m depth, the width at half-height of the (001) illite reflexion reaches again 3.5 mm, like in the upper interval.

6. Discussion

Coming close to the intrusions, smectite disappears, mixed-layered illite–chlorite appears, and finally, near to the intrusion, the mixed-layered illite–chlorite diminishes on behalf of chlorite, which rises. The mineralogical sequence may possibly reflect ascending thermal gradient toward the intrusion and subjacent to the basaltic flow. Thus, the microdoleritic intrusion has a thermal effect on sub- and suprajacent sediments, whereas basaltic flows affect only the bedrock deposits and does not have any effect on cover sediments, deposited after its cooling. A similar example has been described in the Argana basin, Morocco [7].

Magmatic occurrences come with heat and chemical elements income, particularly magnesium. These two factors created changes in the equilibrium conditions of the different mineralogical phases. Detrital argillaceous minerals become metastable under these conditions. New mineral phases, such as chlorite and interstratified illite–chlorite, precipitate from hot fluids. Many authors [4,9,11,20,21] pointed out chlorite presence in hydrothermal environments and attributed it to contact metamorphism. Closer to the intrusion and beneath the basaltic lava flow, illite proportions slightly raise together with an improvement of its crystallinity. Detrital smectite initially present in argillaceous sediments becomes unstable under the new thermal conditions and turns into mixed-layered illite–chlorite. The latter results from the contact between smectite and the magmatic intrusion, as stated by many authors [2,18,21]. Experimental conditions [27] showed the transformation of smectite into mixed-layered illite–chlorite in hydrothermal conditions. During the intrusion and below the basaltic lava flows, new physicochemical conditions prevail. These will enable smectite transformation into mixed-layered illite–chlorite, which itself, in the course of time, turns into more stable chlorite and/or illite. Hydrothermal fluids related to the magmatic activity and the contemporary magmatic rocks alteration by interstitial water strongly heated are presumably enriched with magnesium. The latter is necessary for chlorite formation at the expense of other metastable minerals. In hydrothermal deposits in general, tri-octahedral clays, mainly chlorite and corrensite, may possibly result either from the progressive transformation of a tri-octahedral primary smectite or from direct precipitation from hydrothermal fluids [13]. In RHE3 and MKR3 wells, chlorite (Fig. 9A and B) seems to result from the second mechanism, because the smectites present in the basin are dioctahedral [3,6,12,19,25] and cannot possibly turn into chlorite.

7. Conclusion

The magmatic manifestations of the Upper Cretaceous on the localization and the repartition of the Tunisian eastern margin are directly linked to those of deep fault lanes that enabled basaltic magmas ascension. The emplacement of this magmatism comes along with circulation of hydrothermal fluids; it generated a local geothermal gradient. The sedimentary series of the Upper Cretaceous was locally affected by temperature rise. Income of heat and chemical elements, particularly magnesium, in relation with the placement of magmatic episodes, engendered new clay mineral equilibrium. Dissolution and precipitation by metasomatic mechanisms were induced by the hydrothermal fluids. Detrital argillaceous minerals, such as smectite, became metastable and new hydrothermal phases formed, such as chlorite, which does not exist in the outcrop or in the reference well. Illite crystallinity was improved too.

References

[1] H. Abdallah, Le Crétacé supérieur de la chaîne nord des Chotts (Sud tunisien). Biostratigraphie, sédimentation, diagenèse, thèse, université de Dijon, 1987.

[2] J. Ahn, D.R. Peacor, TEM study of mineralogy and diagenesis of phyllosilicates in volcanogenic sediments from the Southland Syncline, New Zealand, Geol. Soc. Am. Abstr. Prog. 17 (1985) p510.

[3] M. Buattier, A.M. Karpoff, M. Boni, G. Fruh-Green, J. Mc Kenzie, Mineralogical and petrographic records of sediment-fluid interaction in the sedimentary sequence at Middle valley, Juan De Fuca ridge, Proc. Ocean Drilling Program 139 (1994) 133–154.

[4] J.H. Burton, D.H. Krinsley, K. Pye, Authigenesis of kaolinite and chlorite in Texas Golf coast sediments, Clays Clay Miner. 35 (4) (1987) 291–296.

[5] S. Caillère, S. Hénin, M. Rautureau, Minéralogie des argiles, Classification et nomenclature, 2e édition entièrement refondue, 1982.

[6] H. Chamley, J.-F. Deconinck, G. Millot, Sur l'abondance des minéraux smectitiques dans les sédiments marins communs déposés lors des périodes de haut niveau marin du Jurassique supérieur au Paléogène, C. R. Acad. Sci. Paris, Ser. II 311 (1990) 1529–1536.

[7] L. Daoudi, J.-L. Pot de Vin, Effets thermique et hydrothermal de la coulée de basalte triasico-liasique sur les argiles du bassin d'Argana (Maroc), C. R. Geoscience 334 (2002) 463–468.

[8] J. Dercourt, L.P. Zonenshain, L.-E. Ricou, V.G. Kazmin, X. Le Pichon, K.A.L. Nipper, C. Grandjaquet, I.M. Sborschikov, J. Boulin, O. Sorokhtin, J. Geyssant, C. Lepvrier, B. Biju-Duval, J.C. Sibuet, L.A. Savostin, M. Westphal, P. Laver, Présentation de 9 cartes paléogéographiques au 1/20 000 000 s'étendant de l'Atlantique au Pamir pour la période du Lias à l'Actuel, Bull. Soc. geol. France (8) I (1985) 637–658.

[9] A. Drief, F. Nieto, N. Sanchez, Experimental clay-mineral formation from a subvolcanic rock by interaction with 1 M

NaOH solution at room temperature, Clays Clay Miner. 49 (1) (2001) 92–106.
[10] G. Dunoyer de Segonzac, Les minéraux argileux dans la diagenèse, passage au métamorphisme, Mem. Serv. Cart. geol. Als. -Lorr. 29 (1969) 1–320.
[11] N. Ellouze, Étude de la subsidence de la Tunisie atlasique, orientale et de la mer Pélagienne, thèse de 3e cycle, université Paris-6, 1984.
[12] R. Guiraud, J.-C. Maurin, Le *rifting* en Afrique au Crétacé inférieur : synthèse structurale, mise en évidence de deux étapes dans la genèse des bassins, relations avec les ouvertures océaniques péri-africaines, Bull. Soc. geol. France 162 (5) (1991) 811–823.
[13] A. Inoue, M. Utada, Smectite to chlorite transformation in thermally metamorphosed volcaniclastic rocks in the Kamikita area, Northern Honsshu, Japan, Am. Mineral. 76 (1991) 628–640.
[14] M.D. Jouirou, Étude géologique et géotechnique des sédiments de la région d'El Kef (Nord-Ouest de la Tunisie), thèse de 3e cycle, université Bordeaux-1, 1981.
[15] J.I. Junfeng, R.L.P. Browne, Relationship between illite crystallinity and temperature in active geothermal systems of New Zealand, Clays Clay Miner. 48 (2000) 139–144.
[16] N. Laridhi Ouazaa, Étude minéralogique et géochimique des épisodes magmatiques mésozoiques et miocènes de la Tunisie, thèse Es-Sciences, université de Tunis II, 1994.
[17] N. Laridhi Ouazaa, M. Bédir, Les migrations tectono-magmatiques du Trias au Miocène sur la marge orientale de la Tunisie, Africa Geosciences Review 2 (2) (2004) 177–194.
[18] J.H. Lee, D.R. Peacor, D.D. Lewis, R.P. Wintsch, Chlorite-illite/muscovite interlayered and interstratified crystals: A TEM-AEM study, Contrib. Mineral. Petrol. 88 (1984) 372–385.
[19] L. Liangquan, K. Gerta, A. Thiry, W. Stinnesbeck, Late Cretaceous sea-level changes in Tunisia: a multi-disciplinary approach, J. Geol. Soc. Lond. 157 (2000) 447–458.
[20] A. Mas, P. Patrier, D. Beaufort, A. Genter, Clay-mineral signatures of fossil and active hydrothermal circulations in the geothermal system of the Lamentin Plain, Martinique, J. Volcanol. Geotherm. Res. 124 (2003) 195–218.
[21] A. Mas, P. Guisseau, M.-P. Patrier, D. Beaufort, A. Genter, B. Sanjuan, J.-P. Girard, Clay minerals related to the hydrothermal activity of the Bouillante geothermal field (Guadeloupe), J. Volcanol. Geotherm. Res. 158 (2006) 380–400.
[22] H. Mattoussi Kort, L'effet thermique des intrusions magmatiques sur l'encaissant sédimentaire argileux (cas du Crétacé supérieur de la Tunisie orientale), DEA, université Tunis-2, 2003.
[23] H. Mattoussi Kort, Amincissement crustal en Afrique du Nord au cours du Crétacé et manifestations thermiques : domaine oriental de la Tunisie, in: Proc. 3rd Conf. of the Association of African Women Geoscientists, El Jadida, Morocco, 4–13 May 2006, pp. 106–108.
[24] E. Srasra, N. Kebir-Araguib, F. Ayedi, F. Bergaya, H. Van Damme, Mineralogical identification of bentonite clay deposit, J. Soc. Chim. Tunis. VII (7) (1988) 37.
[25] M. Thiry, T. Jacquin, Clay mineral distribution related to rift activity, sea-level changes and paleoceanography in the Cretaceous of the Atlantic Ocean, Clay Miner. 28 (1993) 61–84.
[26] W. Wildi, La chaîne tello-rifaine Algérie, Maroc, Tunisie, structure, stratigraphie et évolution du Trias au Miocène, Rev. Geol. Dyn. Geogr. Phys. 24 (3) (1983) 201–298.
[27] Y.C. Yau, D.R. Peacor, E.J. Essene, J.H. Lee, L.C. Kuo, M.A. Cosc, Hydrothermal treatment of smectite, illite, and basalt to 460 °C: comparison of natural with hydrothermally formed clay minerals, Clays Clay Miner. 35 (4) (1987) 241–250.